SUPPORTING INFORMATION

Structure of an Ancestral Mammalian Family 1B Cytochrome P450 with Increased Thermostability

Aaron G. Bart, Kurt L. Harris, Elizabeth M. J. Gillam, and Emily E. Scott

List of Supporting Information Included:

Table S1. Comparison of salt bridge interactions in extant human CYP1B1 *vs.* the ancestral CYP1B1 enzyme. Red text indicates interactions that are unique to that protein structure. These correspond to the residues show in Figures 6A and 6B, with the exception of partials, which are defined as one are two unique residues that interact with a shared network. Bold indicates that an interaction is between two distinct secondary structure elements. An asterisk indicates that the residue varies between the extant and ancestor enzymes.

Extant Human CYP1B1			
2-residue salt bridges	**Secondary Structure Location**	**Salt-bridge networks**	**Secondary Structure Location**
D116* : H136*	B/B' loop : B'/C loop	E173 : R213: E176 : R175/ H216 : D217	D helix : E/F loop : D helix : E/F loop
E139 : K142	C helix	E223* : H227 : E230*	F helix
D192 : R194*	D/E loop : E helix	**R523 : D361 : R366**	**C-term : J helix : J/J' loop**
R233 : E260*	**F helix : G helix**	R390 : E387 : R444	K helix : K'/ K" loop
E229 : K514	**F helix : $\beta_{4\text{-}2}$ /$\beta_{3\text{-}2}$ loop**	R469 : E473 : K477	K"/L loop : L helix
D274 : R278	G helix	**R145 : HEM : R468/R117 : HEM : H401**	**C helix : HEM : K"/L loop : B/B' loop : K/$\beta_{2\text{-}1}$**
D291 : H279	G/H loop : G helix	**Total : 6 Unique: 1 + 2 partial**	
D316 : K303*	H/I loop : H helix		
E318 : R130	**I helix : B'/C loop**		
D333 : K512	**I helix : $\beta_{4\text{-}2}$**		
D351* : R355	J helix		
D374 : R368	J' helix : J-J' loop		
E438 : H429	K'-K" loop		
Total : 13 Unique: 7			

Ancestral N98_CYP1B1_Mammal			
2-residue salt bridges	**Secondary Structure Location**	**Salt-bridge networks**	**Secondary Structure Location**
R348 : E499	**I helix : β_3 loop**	**R145 : HEM : R468/R117) : HEM : H401**	**C helix : K"/L loop : β/β' loop : K/$\beta_{2\text{-}1}$**
R368 : D374	J/J' loop : J' helix	R444 : E387 : R390	K'/K" loop : K helix
E473 : K477	L helix	**E474 : H149 : R469**	**L helix : C helix : K"/L loop**
E220 : K275	**F helix : G helix**	**D373* : R163 : E167**	**J' helix : D helix**
D274 : R278	G helix	H216 : E176 : R179*	E/F loop : D helix
R290 : D294	G/H loop : H helix	**R523 : D361 : R366**	**C-term : J helix : J/J' loop**
E100 : K433	**B helix : K'/K" loop**	**K416 : D417 : R136***	**$\beta_{2\text{-}2}$/$\beta_{1\text{-}3}$ loop : B'/C loop**
D291 : H279	G/H loop : G helix	**E318 : R130 : D316**	**I helix : B'/C loop : H/I loop**
D333 : K512	**I helix : $\beta_{4\text{-}2}$**	**Total : 8 Unique: 3 + 2 partial**	
E359 : R362*	J helix		
D406* : H413	β_2		
E438 : H429	K'-K" loop		
R213 : E173	E/F loop : D helix		
D504* : K514	β_3/β_4 loop region		
Total : 14 Unique: 6 + 1 partial			

Table S2. Comparison of aromatic and pi-cation stacking interactions in extant human CYP1B1 *vs.* the ancestral CYP1B1 enzyme. Red text indicates interactions that are unique to that protein structure. **These correspond to the residues show in Figures 6C and 6D, with the exception of partials, which are defined as one are two unique residues that interact with a shared network**. Bold indicates that an interaction is between two distinct secondary structure elements. An asterisk indicates that the residue varies between the extant and ancestor enzymes.

Extant Human CYP1B1	
Aromatic or cation-pi stacking interactions	**Secondary Structure Location**
H71 : W425 : H429	**A helix : K′ helix : K′-K″ loop**
F120 : F123 : F134	B-B′ loop : B' helix : B'-C loop
H149 : R153	C helix
F155 : R158*/F156*	C-D loop
F346 : F384	**I helix : K helix**
Y349 : F440	**I/J loop : K′-K″ loop**
Total : 6 Unique: 3 + 1 partial	

Ancestral N98_CYP1B1_Mammal	
Aromatic or cation-pi stacking interactions	**Secondary Structure Location**
W57 : F74	**N-term-β : A helix**
H71 : W425 : H429	**A helix : K′ helix : K'-K″ loop**
R117 : H401	**B-B' loop : K-β2-1 loop**
F123 : F134	B′ helix : B′-C loop
W141 : R468	**C helix : K″-L loop**
H149 : R153	C helix
F231 : F261	**F helix : G helix**
R366 : H489	J-J′ loop
Total : 8 Unique: 5	

Table S3. MRM transitions used for quantification of α-naphthoflavone, metabolites and internal standard.

Compound	Q1	Q3	CE	EP
α-naphthoflavone	273.1	115.1	55	10
	273.1	129.1	55	10
	273.1	143.2	55	10
	273.1	171.2	55	10
	273.1	202.3	55	10
	273.1	226.2	55	10
Progesterone (IS)	315.2	97.1	28	8
	315.2	109.1	28	8
	315.2	297.2	47	8
OH-α-naphthoflavone	289.09	215.09	55	10
	289.09	131.05	55	10
	289.09	115.05	55	10
	289.09	103.05	55	10
	289.09	95.05	55	10
	289.09	77.04	55	10

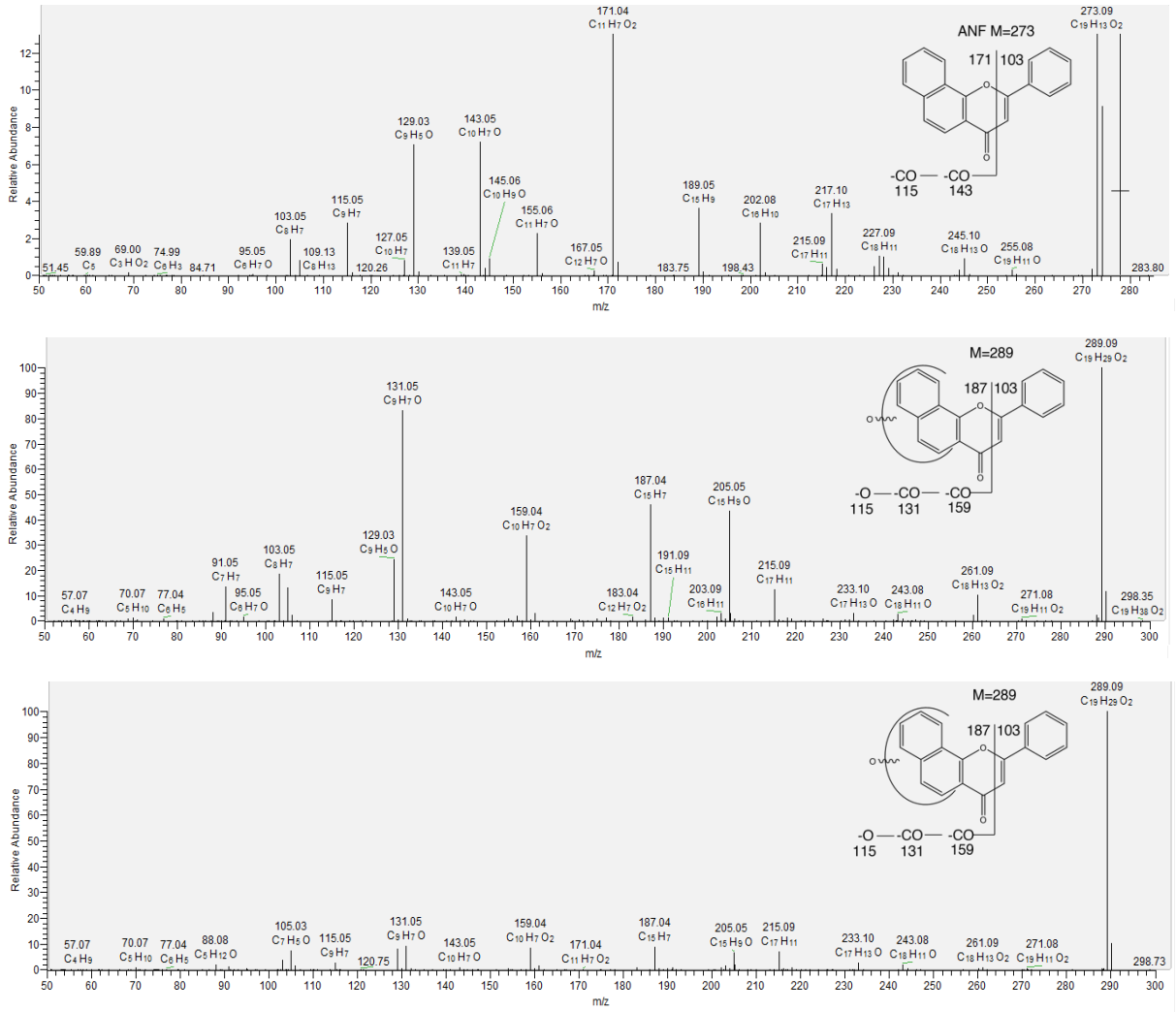

Figure S1. Mass fragmentation of α-naphthoflavone metabolites. Tandem mass spectra and predicted fragmentation patterns of (A) α-naphthoflavone, (B) M1, and (C) M2. The fragmentation patterns of M1 and M2 are consistent with the addition of a single oxygen to the two rings indicated.

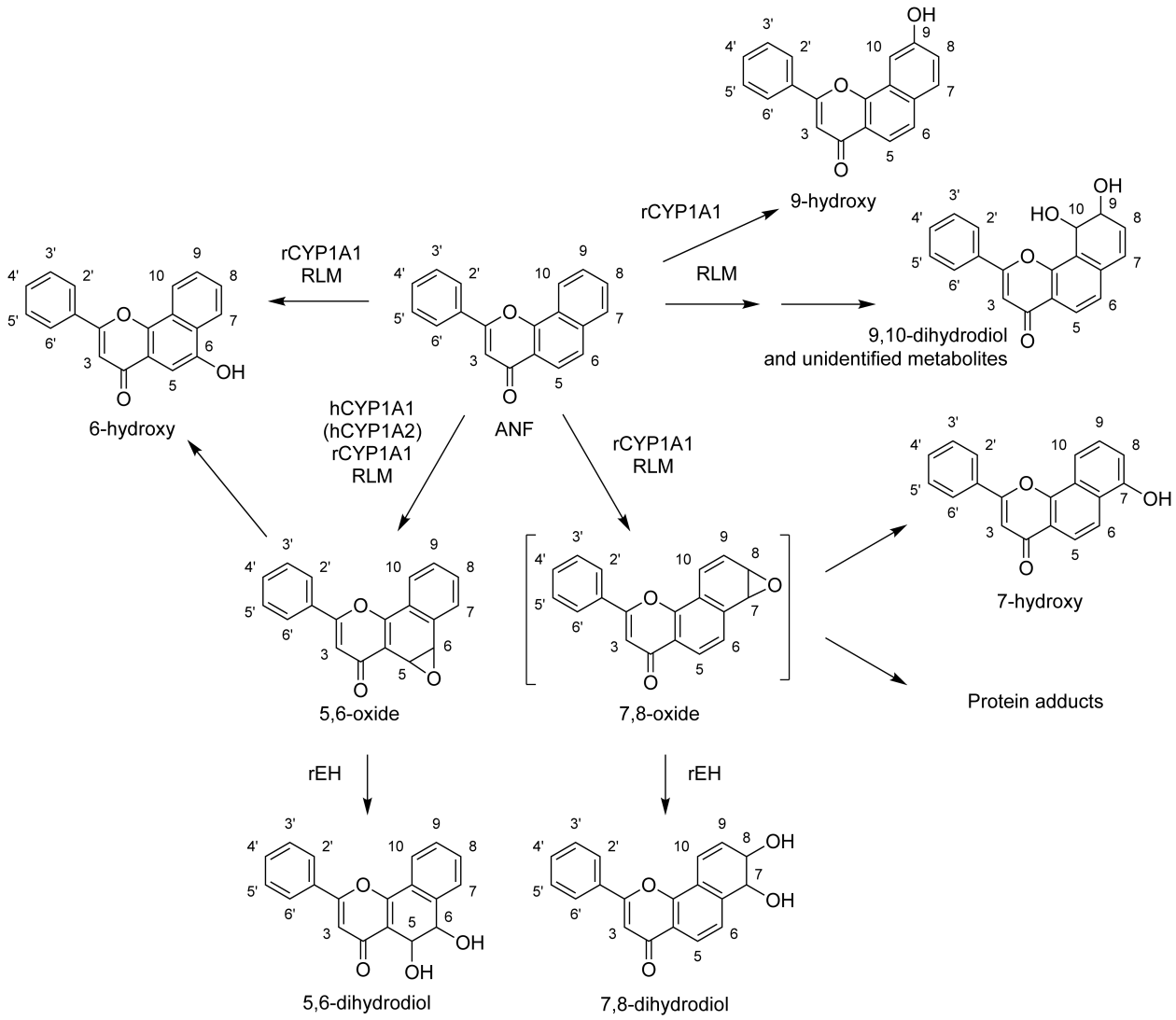

Figure S2. The known metabolic pathways of α-naphthoflavone (ANF) catalyzed by liver microsomes and recombinant CYP1A forms. The known α-naphthoflavone metabolic pathways catalyzed by CYP1 enzymes and rat liver microsomes (RLM) induced by either 2,3,7,8-tetrachlorodibenzodioxin (66), 3-methylcholanthrene, β-naphthoflavone or phenobarbital (67) are summarized. The two main products of α-naphthoflavone metabolism by rat (r)CYP1A1 are the 5,6-oxide and 7,8-oxide (66,67). These compounds are further metabolized by rat epoxide hydrolase (rEH) to form the respective dihydrodiols. In the absence of rEH, the 5,6-oxide is chiefly observed, as the 7,8-oxide is unstable and will interact with nucleophilic groups on proteins, or spontaneously convert to the 7-hydroxy-α-naphthoflavone product (32,68). Recombinant human (h)CYP1A1, and to a lesser extent hCYP1A2, produced the 5,6-oxide as the main product, which was converted to the 5,6-dihydrodiol in the presence of rEH (32). The 7,8-dihydrodiol was not observed even in the presence of rEH. Other minor metabolites produced by recombinant rCYP1A1 or induced RLM are also shown. Earlier studies (69-71) generally agreed with the metabolite assignments shown here, except that the 7,8-dihydrodiol was originally assigned the structure now defined as the 9,10-dihydrodiol.